

# Compensation of Harmonics in Residential Distribution System Using Virtual Impedance

<sup>1</sup>R.Kavin, <sup>2</sup>T.Kesavan, <sup>3</sup>S.Anbumani

<sup>1,2</sup>EEE Department, Sri Krishna College of Engineering & Technology

<sup>3</sup>Bio-Medical Engineering Department, Vellalar College of Engg & Tech

Email: <sup>1</sup>kavin882@gmail.com, <sup>2</sup>t.kesavan87@gmail.com, <sup>3</sup>anbumaniexcel@gmail.com

**Abstract**—this paper presents the modeling of nonlinear load used in domestic and small scale industrial distribution system. Proportional integral controller is used for the current control, fuzzy based MPPT is used for the variation of power from PV due to the change in atmospheric condition. Harmonics are compensated by the virtual impedance implementation. However due to increasing implementation of multiple distributed generation in residential areas, DG grid interfaced converters are used to improve the power quality. Harmonic analysis of the distribution system is used to study the behavior of equipment connected in the non-sinusoidal system environment for designing and optimal location of filters. THD is used as harmonics index to study the effect of these nonlinear loads at utility. In depth analysis and comparison of different compensation schemes based on the virtual harmonic damping impedance concept are carried out. The effect of harmonics and the compensations are verified by the analysis and simulation by MATLAB/Simulink.

**Keywords**— Photo Voltaic, Distributed Generation, Maximum Power Point Tracking, Total Harmonic Distortion, Clean Development Mechanism, Point of Common Coupling.

## 1. INTRODUCTION

The term harmonics referred to Power quality in ideal world would mean how pure the voltage is, how pure the current waveform is in its sinusoidal form. Power quality is very important to commercial and industrial power system designs. Ideally, the electrical supply should be a perfect sinusoidal waveform without any kind of distortion. If the current or voltage waveforms are distorted from its ideal form it will be termed as harmonic distortion. This harmonic distortion could result because of many reasons. In today's world, prime importance is given by the engineers to derive a method to reduce the harmonic distortion. Harmonic distortion was very less in the past when the designs of power systems were very simple and conservative. But, nowadays with the use of non-linear loads in the residential side increases the harmonic distortion.

A grid-connected PV system supplies electricity directly to households, businesses. During daylight hours, the PV panels produce a DC current. This runs through an inverter that converts the current into AC electricity. It is then suitable for electrical appliances and export to the main electricity grid. Unlike traditional 'off-grid' PV systems, grid-connected PV systems require no batteries to store energy. The electricity produced by the PV system is fed into the home's switchboard where it is used to help meet household electricity demand (and offset purchased electricity). If the system produces more electricity than the household is using then electricity is exported to the main electricity grid and the home owner usually receives a credit for that electricity. During peak periods and at night electricity is imported from the grid, as per normal. Whether it is day time, night time, sunny, cloudy, or just a day that can't decide; there will be no flickering of lights or fluctuations to your power supply. The electricity from the PV system simply supplements your existing power supply. Maintenance of a grid-connected PV system is generally limited to ensuring that shade from trees or other obstructions does not become a problem and occasionally checking the panels for dirt and, when necessary, cleaning them with water. The MPPT technique is implemented to track the maximum power from the PV panel and the PID controller is used to track the current in the system to provide control. Unbalance voltage compensation in addition to the primary function of real power injection. This potential for ancillary services can be realized by properly utilizing the available apparent power rating from the

interfacing inverters. Doing so is feasible as most of the time these inverters are not running at their maximum power due to the intermittent nature of renewable energy. The concept of system harmonic compensation using grid interfacing PV inverter has been reported in the literature. Additionally, for a system with distributed loads and DG systems, assigning the harmonic compensation priority to different DG systems to achieve the best compensation result. Then the PV grid-interfacing inverters are connected to the distribution system model and are controlled to improve the power quality by acting as harmonics-damping virtual impedance.

### 1.1 Advantages

The energy which is harvested from the natural resources like sunlight, wind, tides, geothermal Heat etc. is called Renewable Energy. The global energy crunch has provided a renewed impulsion to the growth and Development of Clean and Renewable Energy sources. Clean Development Mechanisms (CDMs) are being adopted by organizations all across the globe. Another advantage of utilizing renewable resources over conventional methods is the significant reduction in the level of pollution associated.

The cost of conventional energy is rising and solar energy has emerged to be a promising alternative. They are abundant, pollution free, distributed throughout the earth and recyclable. PV arrays consist of parallel and series combination of PV cells that are used to generate electrical power depending upon the atmospheric specifics (e.g. solar insulation and temperature).

### 1.2 Disadvantages

The temperature from the sun is not available all time to generate the required power to meet the demand. Due to the varying atmosphere the power produced from the PV also get varied. This power can't send to the load directly. We have to control this to attach the PV pane to the load. Grid is a voltage source of infinite capability. The output voltage and frequency of inverter should be same as that of grid frequency and voltage. When PV is connected to the grid the grid standards are affected.

### 1.3 Application

Solar technologies are broadly qualified as either passive or active depending on the way they catch, change over and distribute sunlight. Active solar proficiencies use photovoltaic arrays, pumps, and fans to convert sunlight into executable outputs. Passive solar techniques include selecting materials with favorable thermal attributes, and citing the position of a building to the Sun. The standalone PV Systems have been used for solar street lighting, home lighting system, SPV water pumping system. A hybrid system installed with a backup system of diesel generator can be used in remote military installations, health centers and tourist bungalows. In grid connected system the major part of the load during the day is supplied by the PV array and then from the grid when the sunlight is not sufficient.

The paper is organized in an order such as to provide the readers with a general understanding of the different components present in the photovoltaic battery charging system with maximum power point tracker, before moving on to the details specific to the paper.

## 2. VIRTUAL IMPEDANCE COMPENSATION

In this paper, the PV inverters are controlled as virtual harmonic impedance at the harmonic frequencies to compensate

the residential system harmonics. Therefore, before the residential system model and harmonic compensation performances are discussed, the virtual impedance control concept is introduced in this section. Virtual impedance emulates the effect of physical impedance, without the need to connect any physical component to the system. In the DG inverter control, the virtual impedance is implemented by modifying the voltage or current reference or the PWM signal, through digital control of the inverters. Virtual impedance can be either at the fundamental frequency or at the harmonic frequencies. The fundamental frequency virtual impedance is used mainly to facilitate DG power flow control and grid disturbance ride through. The harmonic virtual impedance is mainly used for active damping and distribution system harmonic compensation. This thesis is focused on the system harmonics compensation using PV inverters, the virtual harmonic impedance and two subsections. In this two subsection the virtual inductor is discussed briefly for control operation because in the harmonic resistance technique the drop in voltage occurs due to the resistance effect.

Distribution system harmonics improvement using a current controlled grid-interfacing inverter is discussed. In this method, the DG operates like a shunt active power filter (APF) and absorbs the harmonic current generated by the nonlinear load. As a result, the source current becomes harmonic free and the PCC voltage total harmonic distortion (THD) decreases. A popular way to achieve this function is to operate the DG as resistive-APF (R-APF) Here, the harmonic components of the grid side voltage are extracted and the reference harmonic current of the DG is produced by using. As a result, the DG acts as a virtual resistance, only at the harmonic frequencies A harmonic compensation method by a voltage-controlled DG unit is proposed in , where the DG unit is represented as a controlled voltage source with output series impedance. The harmonic components of the controlled voltage source are controlled according to the harmonic voltage of the point of common coupling (PCC) with a positive feedback gain. As a result, the equivalent harmonic impedance of the DG becomes

$$Z_{DG}/(1+G) \quad (2.1)$$

Virtual inductive equivalent impedance is introduced in this method to compensate the system harmonics, since the impedance is mainly inductive at harmonic frequencies. This method is quite attractive for use in a micro grid. Voltage-controlled DG is important for providing the micro grid voltage and frequency control.  $G$  is the feedback gain. The harmonic voltage is controlled by PCC voltage such as,

$$V_{DG} = -G \times V_{PCC} \quad (2.2)$$

The virtual impedances act like real impedances for unbalanced loads or unbalanced voltages, as the negative sequence current will cause the same imbalance voltage drop. However, if necessary, the virtual impedance based negative sequence and the harmonic currents sharing methods can also be implemented to further improve micro grid power quality when significant harmonic and unbalanced loads present.

After obtaining the virtual impedance voltage drop, this voltage drop shall be incorporated into the voltage control loop of the DG inverters. Fig. 4.1 shows the overall voltage control diagram of an interfacing inverter. As shown, the reference voltage comes from the power control loop, and the virtual impedance voltage drop is subtracted from the reference voltage to produce the virtual impedance effects. For the DG system with an output LC filter, a multi loop voltage control scheme is adopted, where the output loop uses a PI controller. However, in a microgrid with significant harmonic loads, it is preferred to use multiple harmonic resonant controllers at harmonics. For the inner loop, a proportional controller  $K_{ind}$  (gain) is employed. To evaluate the closed-loop dynamic characteristics of the voltage control, the interfacing converter can be modeled by the Thevenin equivalent circuit as expressed in

$$VDG(s) = G(s) \cdot Vref(s) - Zout(s) \cdot I(s) \quad (2.3)$$

Where,

$VDG(s)$  and  $Vref(s)$  are the actual and reference DG voltages,

$I(s)$  is the DG current,

$G(s)$  is the close-loop voltage control gain, and

$Zout(s)$  is the impedance introduced by the DG voltage control.

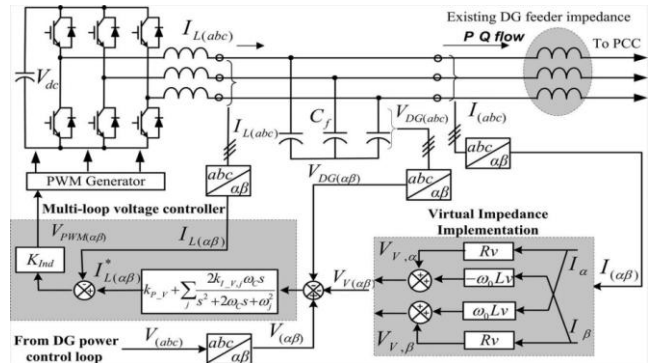


Figure 2.1 Voltage control and virtual impedance implementation.

Properly controlling the DG harmonic voltage with a positive feedback gain of  $G$ , the DG harmonic impedance will be scaled down by a factor of  $(1+G)$ . Therefore, the harmonic impedance at the DG side can be substantially lower than that at the grid side. As a result, most of the nonlinear load current will be absorbed by the DG unit, leaving an improved grid current and PCC voltage. Obviously, a higher  $G$  value will further reduce the PCC voltage harmonics.

With  $G = 0$ , the system will be a standard voltage-controlled DG unit without any active compensation. The harmonic current can be shared automatically according to the DG- and grid-side harmonic impedances.

This is in contrast to the current-controlled method, where the DG current will be sinusoidal if the active power filtering function is not enabled. Since a high value of  $G$  tends to have over modulation problems and makes the system unstable, a practical top limit of  $G$  should be selected carefully. Finally, it is important to note that  $G$  should not be less than  $-1$ , as this will introduce capacitive equivalent impedance, which may induce some system resonance. In this work,  $G > 0$  is named as harmonic compensation mode,  $G = 0$  is named as uncontrolled mode, and  $G < 0$  is defined as harmonic rejection mode.

### 3. DG HARMONIC COMPENSATION AND NONLINEAR LOADS

The harmonic compensation effects using PV inverters are discussed in this topic. Residential PV system locations are usually not controllable as they depends on which residence has the system installed. However, coordinated control of the PV inverters in a system is possible, and an optimal compensation strategy should be identified to obtain the best harmonic compensation result. The two strategies for harmonic compensation using the DG interfacing inverters are the end-of-distribution-feeder compensation, and distributed compensation. In a distribution system with multiple PV systems, the end-of-line compensation strategy can be implemented by assigning harmonic compensation priority to the PV inverters connected at the end of the feeder. On the other hand, the distributed compensation approach can be implemented by operating all PV inverters in the harmonic compensation mode with equal priority.

Harmonic impedance consists of the negative inductances and the positive resistances at the dominant harmonic frequencies, which can be given by

$$\begin{pmatrix} V^* \alpha_{ahp} \\ V^* \alpha_{\beta hp} \end{pmatrix} = \begin{pmatrix} R_{hp} & -\omega_{hp} L_{hp} \\ \omega_{hp} L_{hp} & R_{hp} \end{pmatrix} \begin{pmatrix} i_{\alpha hp} \\ i_{\beta hp} \end{pmatrix}$$

$$\begin{pmatrix} V^* \alpha_{ahn} \\ V^* \alpha_{\beta hn} \end{pmatrix} = \begin{pmatrix} R_{hn} & \omega_{hn} L_{hn} \\ -\omega_{hn} L_{hn} & R_{hn} \end{pmatrix} \begin{pmatrix} i_{\alpha hn} \\ i_{\beta hn} \end{pmatrix} \quad (3.1)$$

Where the terms "hp" and "hn" are used to denote the positive sequence harmonic components and the negative-sequence harmonic components, respectively. To study the effects of different compensation approaches, a two-node system is used as an example. To simplify the analysis, it is assumed that both node 1 and 2 have identical loads (the same

line parameters, and the same transformers). Then the equivalent circuit for analysis is formed. In this case, we can take and as the state variables, to be the input, and to be the output of the state space model of the system. Using the distribution system modeling technique are derived in the term  $v/i$ . The harmonic compensation at a single node (node 1 or node 2) will better damp the harmonic voltage at node 1 compared to distributed compensation for (here, represents the harmonic order). However, when distributed compensation provides better damping at node 1. A similar observation is true for node 2 voltage as shown in Fig. which reveals that the distributed compensation method provides better harmonic damping in the high-frequency region. Therefore the decision about the optimal compensation strategy can be different depending on the dominant harmonics of the load.

This frequency-related performance of different compensation methods can be intuitively explained by the equivalent circuit. At high frequencies, the impedances are much higher than the inverter virtual harmonic impedance. As a result, if  $Z_{rh}$  are connected, most of the adjacent harmonic load current will flow through  $Z_{rh}$ . For example, in the case of DG at node 1 [Fig. 11(a)], most of will be absorbed by  $Z_{rh}$ , but will flow through  $Z_{rh}$  nodes 1 and 2. This process will result in a higher  $Z_{rh}$  at nodes 1 and 2. The situation will be similar when a single DG is at node 2. However in the case of DG at both nodes 1 and 2 most of the harmonic content of  $Z_{rh}$  will be locally absorbed by  $Z_{rh}$  and respectively. As a result, the voltages at nodes 1 and 2 will be less polluted. When the harmonic frequency increases and  $Z_{rh}$  also increases but the virtual resistance  $Z_{rh}$  remains the same, providing the same level of damping to the load harmonics. This result also explains the constant damping at the high frequency range in the case of DG at nodes 1 and 2. (Another observation from Fig. 10(a) and (b) is that, at high frequencies the gain of  $Z_{rh}$  is almost identical for DG at node 1 or node 2, but has a lower gain in the case of DG at node 2 compared to the gain at node 1. The reason is that, regardless of the DG location (node 1 or 2), the harmonic current flowing to node 1 is almost identical in both cases (especially since the feeder impedance is lower than the transformer impedance with). However, in the case of DG at node 2, the harmonic current flowing through  $Z_{rh}$  is much lower. In this case, most of  $Z_{rh}$  is absorbed by  $Z_{rh}$ , and most of  $Z_{rh}$  flows through grid side impedance. The closed-loop dynamic behavior of inverter voltage control system can be described as follows

$$V_o(s) = G_{cl}(s) V_o^*(s) - Z_o(s) I_o(s) \quad (3.2)$$

$Z_h(s)$  is the synthesized harmonic impedance, which can be described in the stationary frame as

$$Z_h(s) = \sum \frac{2\omega_c(R_h S - (h\omega_f)^2 L_h)}{s^2 + 2\omega_c s + (h\omega_f)^2} \quad (3.3)$$

For the compensation at a low-frequency range, the virtual damping resistances of DGs are comparable to  $Z_{rh}$ . Therefore, more harmonic current will flow to the source through the feeders, causing relatively high harmonic voltages in the system.

$$HBPF(s) = HLPF \left( \frac{s^2 + (h\omega_f)^2}{2s} \right) \Rightarrow \frac{2\omega_c s}{s^2 + 2\omega_c s + h\omega_f^2} \quad (3.4)$$

Where  $\omega_c$  is the cutoff frequency of the LPF in the multiple rotating reference frames, which in this case has a bandwidth of 1 Hz. With this transformation, the effect of the  $Z_h(s)$  can be analyzed in the closed-loop transfer function. The cutoff frequency is calculated for the bode plot of the system then the compensation is chosen depending upon the crossover frequency. The system frequency below the cross over frequency the end off line compensation will choose. The frequency above the cross over frequency the distributed compensation is used.

Figure 3.1 reveals that harmonic compensation at a single node will better damp the harmonic voltage at node compared to distributed compensation for  $h < \text{fundamental frequency}$ . However, when  $h > \text{fundamental frequency}$  distributed

compensation provides better damping at node, which reveals that the distributed compensation method provides better harmonic damping in the high-frequency region. Therefore the decision about the optimal compensation strategy can be different depending on the dominant harmonics of the load. The above analysis results were obtained from a simple 2-node distribution system. The analysis is extended to a more practical 11-node system in the future work.

Bode Diagram

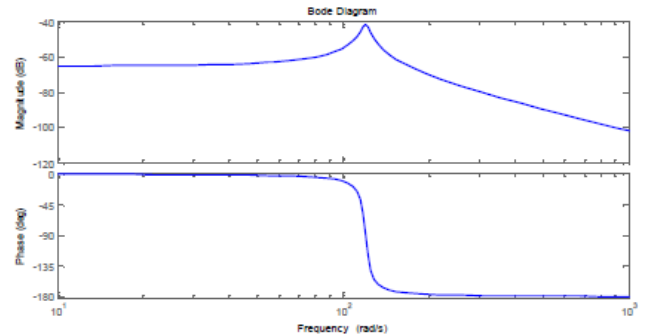


Figure 3.1 Frequency-domain responses of the designed harmonic impedances

### 3.1 NONLINEAR LOAD DESIGN

It develops individual units of consumers developed, which are a certain combination of electric device models. These units are called with terms “home” and “office”. These models are obtained using statistical data about different residential regions in Iran. In the simplest case, a home is a combination of four lighting loads and one induction motor. Fig 3.2 & 3.3. shows this consumer unit simulated in Simulink.

There are many reasons for the importance given to the power quality. One of the main reasons is, the consumers are well informed about the power quality issues like interruptions, sagging and switching transients. Also, many power systems are internally connected into a network. Due to this integration if a failure exists in any one of the internal network it would result into unfavorable consequences to the whole power system. In addition to all this, with the microprocessor based controls, protective devices become more sensitive towards power quality variation than were the past generation protective devices.

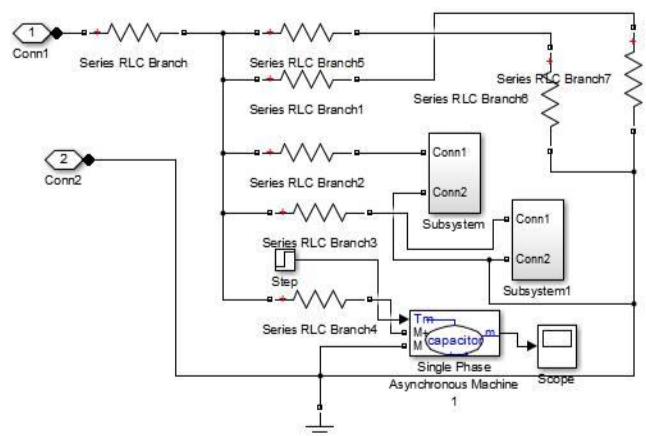


Figure 3.2 Home unit with two CFLs, two lamps and induction motor.

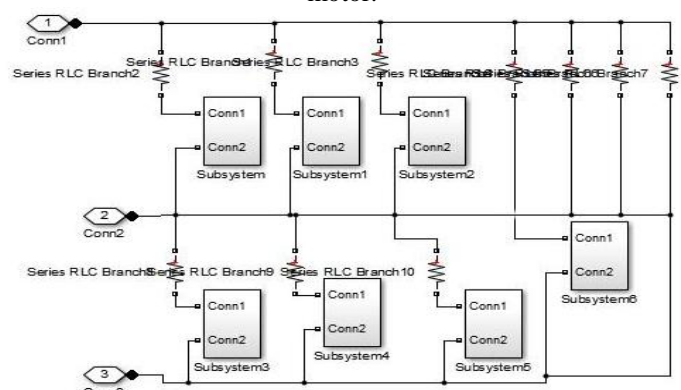


Figure 3.3 shows a sample commercial (office) consumer unit. Eddy current loss of transformer core depends on the squares of both current and frequency. Therefore, the core loss for different experiments is compared to each other using equation  $f_{h1}$  and  $f_{h2}$  correspond to the frequency components of

the different cases in comparison. A similar approach is used for the hysteresis effect. However, hysteresis effect comparison is a new approach is presented for the analysis of switch mode devices and their effect on distribution network. In this approach, model of electronic devices are derived from detailed circuit simulation and the results are transformed to a circuit model which is a combination of passive current circuits. The model contains the odd harmonics of the power system frequency. Based on this model, we developed a probabilistic model for the electronic device and used numerical calculation to estimate the probability distribution of the power system current as a whole. This model shows that adding electronic devices to the power system must be carefully planned so that the power system KPI does not exceed the recommended levels. This stochastic simulation is a strong tool to evaluate the situation of the power system and its capacity for growth.

In case of mass use of electronic devices, additional capacity must be provided both for transformers and distribution lines, in order to avoid harms in the network via harmonic mitigation. We also presented a list of the power system KPI and the devices that can be affected by the additional current harmonics. We classified the equipment into the feeding and consuming sides and studied the effects on each side separately. Mass usage of switch mode devices in different power systems must be planned carefully in order to avoid any unexpected negative effects on the other equipment in the system. The most vulnerable equipment of the power system is the ones which contain solenoids, such as transformers and measurement equipment, especially on the feeding side. Therefore, extra care and calculations are required in different power systems for a safe use of electronic devices. Electronic devices are affected by the harmonic distortion and may need to be either equipped with protective filters or be replaced by more advanced ones. Based on the power system KPI and the specification of the distribution and consumption devices we can use the stochastic analysis approach for dimensioning an optimal power system with respect to equipment costs and safety margins.

#### 4. SIMULATION AND RESULTS

Simulation is the imitation of the operation of a real-world process or system over time. The act of simulating something first requires that a model be developed; this model represents the key characteristics or behaviors/functions of the selected physical or abstract system or process. The model represents the system itself, whereas the simulation represents the operation of the system over time. Simulation is used in many contexts, such as simulation of technology for performance optimization, safety engineering, testing, training, education, and video games. Often, computer experiments are used to study simulation models. Simulation is also used with scientific modeling of natural systems or human systems to gain insight into their functioning. Simulation can be used to show the eventual real effects of alternative conditions and courses of action. Simulation is also used when the real system cannot be engaged, because it may not be accessible, or it may be dangerous or unacceptable to engage, or it is being designed but not yet built, or it may simply not exist. Key issues in simulation include acquisition of valid source information about the relevant selection of key characteristics and behaviors, the use of simplifying approximations and assumptions within the simulation, and fidelity and validity of the simulation outcomes.

##### 4.1 Parameters used in the MATLAB Code

The values of the parameters used in developing the MATLAB code for the Photovoltaic array have been tabled below. The values for the voltage, current, frequency, PV panel temperature are shown in the tabulation below.

Parameter		Value
LC Filter	Filter inductor	$L=5\text{mH}; R=0.2$
	Filter capacitor	40 $\mu\text{F}$
Outer Loop	Cut off frequency	4rad/s
	Proportional gain	0.22
	Resonant gain	25
	Fundamental frequency	120 $\pi$ rad/s
Inner Loop	Inner loop gain	22
	Dc link voltage	230 V
Power Circuit	Switching frequency	4.5KHZ
	$N_p$	12
No .Of Cells In Series	$N_s$	32
Constant	$K_i$	25 C
Temperature	$Tr1$	0.00023A.K
Constant	A	2.15
Charge	Q	1.6022*10 <sup>-19</sup> C

Table 7.1 parameters used in MATLAB/SIMULINK

##### 4.2 Simulation Model

Fig 4.1 shows that PV grid interfaced inverter with virtual impedance technique. The simulation diagrams consist of PV, MPPT, converter, inverter, grid, load, virtual effect creation by the comparison of fundamental voltage or current. DC output from the PV panel is connected to the DC-DC converter (boost) circuit to boost the DC from the PV panel. MPPT block is connected between the PV and DC-DC converter to track the maximum power from the PV.

The gate pulse generated from the MPPT is given to the DC-DC converter. Depending upon the gate signal given to the switch connected to the converter, the voltage is boosted (ex; 35.5 V dc is boosted and converted to 127V ac). The boosted DC is converted in to AC by the DC-AC inverter.

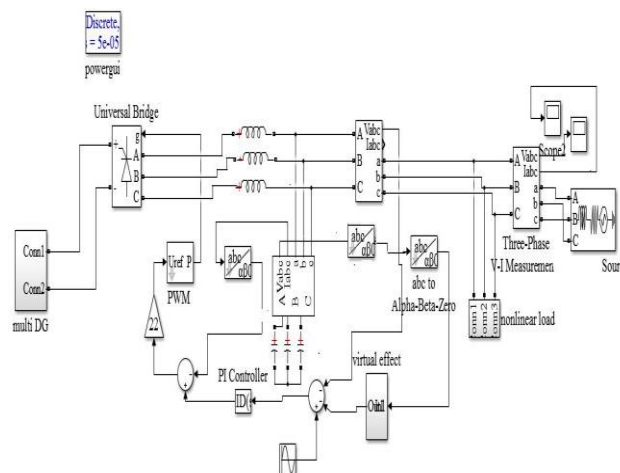


Figure 4.1 simulation of PV grid interfaced inverter with virtual impedance.

Then LC filter is connected to the inverter to filter the output from the inverter. Then it will be connected to the grid and the load. When the system connected to the grid, compensation technique is needed to maintain the grid standards.

The performance of the each block connected in the simulation results is discussed in 4.2.1. The output voltage with and without compensation, gate pulse of MPPT to the converter, shown below.

##### 4.2.1 Performance of PV module

It is observed that by increasing the solar isolation level, the power from Figure 4.2.

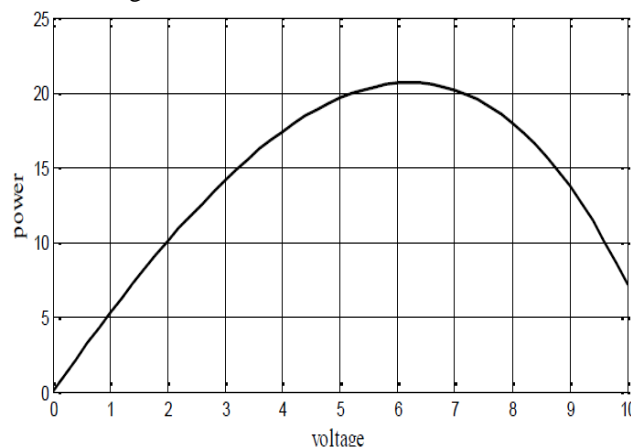


Figure 4.2 PV characteristics of PV Module

From the fig 4.3 it is clearly observed that the boost converter steps up the voltage from 10 to 20 volt in accordance with the parameters derived earlier, fulfilling the desired conditions of output current being 0.4 A at frequency 50kHz. The efficiency of the boost converter is 94.16%. The frequency of operation is 50 kHz. The output current obtained from simulation, which is 0.4 A. The output voltage obtained from simulation, which is 15 V. Duty Cycle is maintained above 20%.

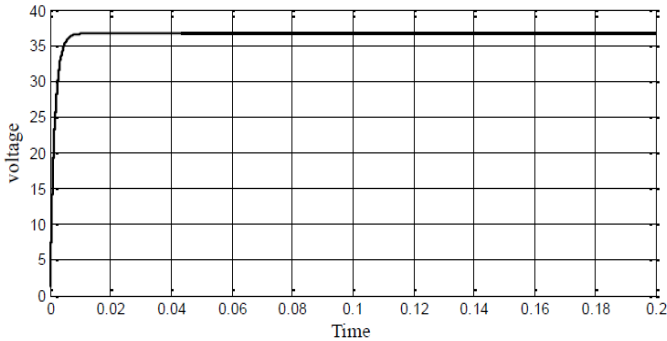


Figure 4.3 output Voltage of Converter

#### 4.2.2 Performance of fuzzy based MPPT:

The pulse to the switch in the DC-DC converter is generated by the MPPT. Fig shows 4.4 that the gate pulse to the switch connected to the DC-DC converter. This pulse generated by the IC algorithm. In this algorithm the maximum power from the PV is tracked in the fast varying atmospheric condition by calculate the present and past voltage and current. The gate pulse generated by the MPPT is given to the boost circuit switch. Due to the switch pulses the converter get the constant maximum power from the PV even in the fast varying atmospheric condition.

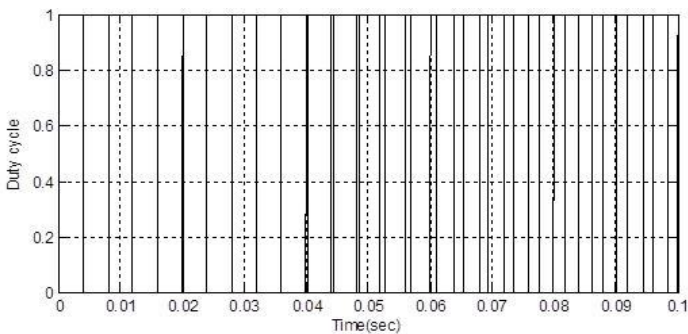


Figure 4.4 Duty Cycle of MPPT

In X -axis mention the time and in the Y -axis voltage range. The distortion from the output is compensated by connecting the virtual impedance technique. Without virtual impedance compensation the system voltage is distorted from the fundamental. The THD range of the system reaches high value than the rated value.

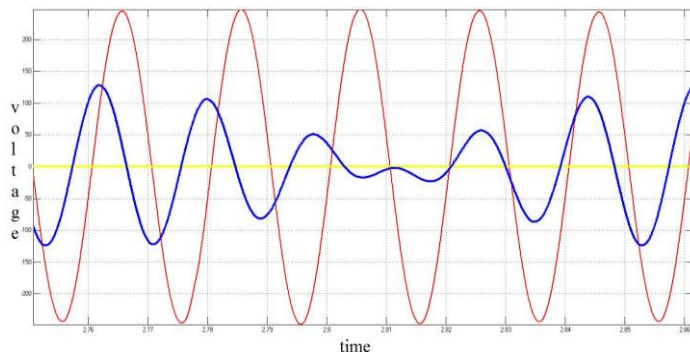


Figure 4.5 output voltage without virtual impedance compensation

The system without virtual impedance compensation is not performed well , the component are connected physically to the system to provide the compensation in the other types of compensation and the components cost and effect created by this equipment also considered for the proper compensation. Also the operation of the equipment depends the some factor if any change occurs in that the total operation provided by this equipment affected. The output for this kind of operation is shown figure 4.5.

At first, the performance of DG1 in grid-connected operation is investigated. In this test, the DG impedance is controlled within the designed range, therefore the stability and small disturbance rejection ability shall be guaranteed. The reactive power (Q-a) decreases to around 10 Var during the transient. The reactive power coupling disturbance is reduced by around 75%, while the dynamics of real power tracking is maintained to be the same. Note that although the real power is slightly affected, the power disturbance is only around 15 W, and it can be stabilized rapidly. Depending on the reactive power difference, the virtual impedance is regulated adaptively to ensure a fast reactive power tracking. As discussed previously, when the reactive power transient completes, the virtual reactance and resistance restore slowly to their originally designed values. Therefore, the virtual impedance restoration process does not cause any power oscillations. The performance of the DG system during 9% grid voltage sags. Therefore, the current surge during grid voltage sag is reduced obviously. After the transient, the transient impedance also goes back to its original value automatically.

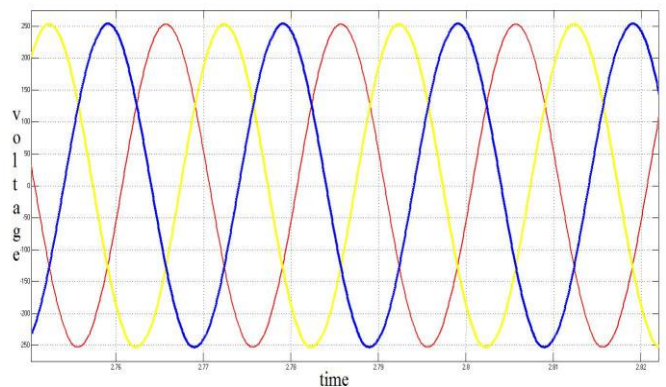


Figure 4.6 output voltage with virtual impedance compensation.

The results are taken for the single DG system only it can be derived for the other DG systems connected. When the fixed virtual impedance is adopted in the simulation, the peak-to-peak current is around 19.5 A. As expected, when the disturbance ride-through function is enabled in Fig. 7.6, the impedance ( $\omega L$  ( $LV + \Delta LV$ ), ( $RV + \Delta RV$ )) can be tuned according to line current magnitude.

The results are taken for the single DG system only it can be derived for the other DG systems connected. When the fixed virtual impedance is adopted in the simulation, the peak-to-peak current is around 19.5 A. As expected, when the disturbance ride-through function is enabled in Fig. 7.6, the impedance ( $\omega L$  ( $LV + \Delta LV$ ), ( $RV + \Delta RV$ )) can be tuned according to line current magnitude. Analysis of the waveform as shown, found the total harmonic distortion (THD) is approximately at 90.27%. When subjected to compensation, the waveform is now continuous, almost sinusoidal and in phase with the supply voltage. Refer to Fig. 7.7 visually shown that when employs virtual impedance technique the supply waveform become smoother and low ripple compared to hysteresis. In addition, the THD level is reduced from 2.65% when apply virtual resistance to 0.68% using virtual inductor .Total harmonic distortion is calculated by the ratio between the harmonic voltage to the fundamental voltage.

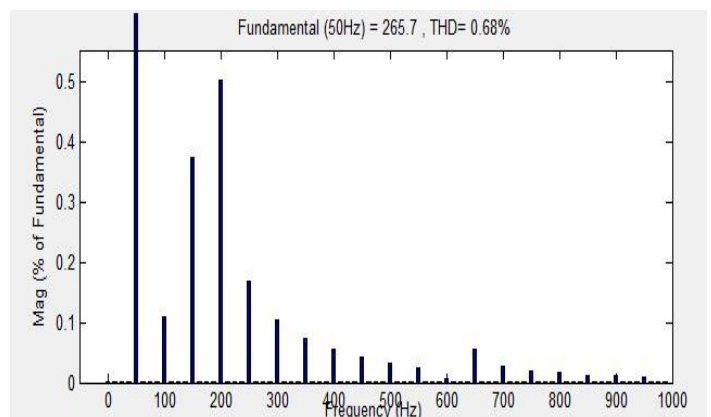


Figure 4.7 THD Analysis of Output Voltage

Analysis of the waveform as shown, found the total harmonic distortion (THD) is approximately at 90.27%. When

subjected to compensation, the waveform is now continuous, almost sinusoidal and in phase with the supply voltage. Refer to Fig. 4.8 visually shown that when employs virtual impedance technique the supply waveform become smoother and low ripple compared to hysteresis. In addition, the THD level is reduced from 3.65% when apply virtual resistance to 2.41% using virtual inductor.

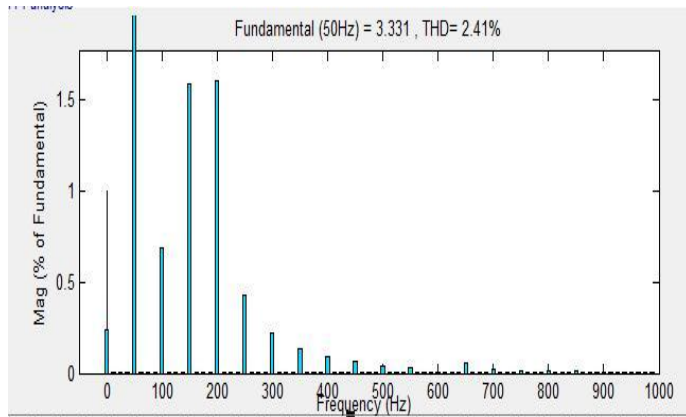


Figure 7.8 THD analysis of Output Current

## 5. CONCLUSION

In this paper design of DG impedance and implementation approach was carried out. In addition, an adaptive transient virtual impedance control method and a transient impedance voltage drop feed forward compensation scheme are proposed to further improve the performances of DG units in a grid-connected micro grid. Experiments are conducted to prove the proposed design, implementation approach, and control strategies. Specifically, the analysis and simulation results showed that the end-of-line compensation provided better damping for low order harmonics, whereas distributed compensation provided better damping for high-order harmonics if the equal equivalent rating of the DG was maintained. We explored the idea of using residential system DG-grid interfacing inverters as virtual harmonic impedance to damp the system harmonics and improve the power quality. In the literature the virtual resistance technique is used to provide compensation but, in this thesis virtual inductor is taken for the compensation. The THD level is decreased from 2.6% to 0.68 in voltage and 2.41% in current. After such a determination has been made, proper priorities can be assigned to the inverters in the distribution system for optimal compensation performance. The fuzzy based MPPT technique are used to track the maximum power from the PV panel and give the gate signal to the boost circuit. In this project 5<sup>th</sup> & 7<sup>th</sup> order harmonics are compensated.

In future work, it considers a supervisory control system of the DGs with communication in order to control the participation from each PV inverter automatically according to the identified priority. Also, to provide an accurate effectiveness analysis of the harmonics compensation by using PV inverters throughout the day/season/year, the use of a statistical home model of a residential system and solar irradiance historic data could also be considered.

## REFERENCES

- i. M. Prodanovic, K. D. Brabandere, J. V. D. Keybus, T. Green, and J. Driesen, "Harmonic and reactive power compensation as ancillary services in inverter-based distributed generation," *IEEE Proc. Gener. Transm. Distrib.*, vol. 1, no. 3, pp. 432–438, May 2007.
- ii. P. T. Cheng and T. L. Lee, "Distributed active filter systems (DAFSs): A new approach to power system harmonics," *IEEE Trans. Ind. Appl.*, vol. 42, no. 5, pp. 1301–1309, Sep.–Oct. 2006.
- iii. T. L. Lee, J. C. Li, and P. T. Cheng, "Discrete frequency tuning active filter for power system harmonics," *IEEE Trans. Power Electron.*, vol. 24, no. 5, pp. 1209–1217, May 2009.
- iv. Y. W. Li and C. N. Kao, "An accurate power control strategy for power electronics-interfaced distributed generation units operating in a low voltage multi bus micro grid," *IEEE Trans. Power Electron.*, vol. 24, pp. 2977–2988, Dec. 2009.
- v. J. He and Y. W. Li, "Analysis, design and implementation of virtual impedance for power electronics interfaced distributed generation," *IEEE Trans. Ind. Appl.*, vol. 47, pp. 2525–2538, Nov./Dec. 2011.
- vi. D. M. Vilathgamuwa, P. C. Loh, and Y. W. Li, "Protection of micro grids during utility voltage sags," *IEEE Trans. Ind. Electron.*, vol. 53, pp. 1427–1436, Oct. 2006.
- vii. J. He, Y. W. Li, D. Bosnjak, and B. Harris, "Investigation and active damping of multiple resonances in a parallel-inverter based microgrid," *IEEE Trans. Power Electron.*, vol. 28, no. 1, pp. 234–246, Jan. 2013.
- viii. J. He, Y. Li, and S. Munir, "A flexible harmonic control approach through voltage controlled DG-grid interfacing converters," *IEEE Trans. Ind. Electron.*, vol. 59, no. 1, pp. 444–455, Jan. 2012.
- ix. R. Dwyer, A. K. Khan, M. Mcgranaghan, L. Tang, R. K. Mccluskey, R. Sung, and T. Houy, "Evaluation of harmonic impacts from compact fluorescent lights on distribution systems," *IEEE Trans. Power Syst.*, vol. 10, no. 4, pp. 1772–1779, Nov. 1995.
- x. E. J. Currence, J. E. Plizga, and H. N. Nelson, "Harmonic resonance at a medium-sized industrial plant," *IEEE Trans. Ind. Appl.*, vol. 31, no. 4, pp. 682–690, Jul./Aug. 1995.
- xi. H. D. Chiang, J. C. Wang, O. Cockings, and H. D. Shin, "Optimal capacitor placements in distribution systems: Part I and part II," *IEEE Trans. Power Del.*, vol. 5, no. 2, pp. 634–649, Jan. 1990.
- xii. D. P. Hohm and M. E. Ropp, "Comparative Study of Maximum Power Point Tracking Algorithms," *Progress in photovoltaic: research and applications*, 2003, vol. 11, pp. 47–62, 2003.
- xiii. Yang, S.; Lei, Q.; Peng, F.Z.; Qian, Z. A robust control scheme for grid-connected voltage source inverters. *IEEE Trans. Power Electron.* 2011, 58, 202–212.
- xiv. J. M. Guerrero, L. G. Vicuna, J. Matas, M. Castilla, and J. Miret, "Output impedance design of parallel-connected UPS inverters with wireless load sharing control," *IEEE Trans. Ind. Electron.*, vol. 52, no. 4, pp. 1126–1135, Aug. 2005.
- xv. E. A. A. Coelho, P. C. Cortizo, and P. F. D. Garcia, "Small signal stability for single phase inverter connected to stiff ac system," in *Conf. Rec. IEEEIAS Annu. Meeting*, Oct. 1999, vol. 4, pp. 2180–2187.
- xvi. D. N. Zmood and D. G. Holmes, "Stationary frame current regulation of PWM inverters with zero steady-state error," *IEEE Trans. Power Electron.*, vol. 18, no. 3, pp. 814–822, May 2003.
- xvii. J. M. Guerrero, L. Hang, and J. Uceda, "Control of distributed uninterruptible power supply systems," *IEEE Trans. Ind. Electron.*, vol. 55, no. 8, pp. 2845–2859, Aug. 2008.
- xviii. J. He, Y. W. Li, D. Bosnjak, and B. Harris, "Investigation and active damping of multiple resonances in a parallel-inverter based microgrid," *IEEE Trans. Power Electron.*, vol. 28, no. 1, pp. 234–246, Jan. 2013.
- xix. Y. W. Li, "Control and resonance damping of voltage source and current source converters with LC filters," *IEEE Trans. Ind. Electron.*, vol. 56, pp. 1511–1521, May 2009.
- xx. J. He, Y. Li, and S. Munir, "A flexible harmonic control approach through voltage controlled DG-grid interfacing converters," *IEEE Trans. Ind. Electron.*, vol. 59, no. 1, pp. 444–455, Jan. 2012.